Astronomy
&
Astrophysics

Lifetime of OH masers at the tip of the asymptotic giant branch

D. Engels and F. Jiménez-Esteban[*]

Hamburger Sternwarte, Gojenbergsweg 112, 21029 Hamburg, Germany
e-mail: dengels@hs.uni-hamburg.de

ABSTRACT

Context. A large fraction of otherwise similar asymptotic giant branch stars (AGB) do not show OH maser emission. As shown recently, a restricted lifetime may give a natural explanation as to why only part of any sample emits maser emission at a given epoch.
Aims. We wish to probe the lifetime of 1612 MHz OH masers in circumstellar shells of AGB stars.
Methods. We reobserved a sample of OH/IR stars discovered more than 28 years ago to determine the number of stars that may have since lost their masers.
Results. We redetected all 114 OH masers. The minimum lifetime inferred is 2800 years (1σ). This maser lifetime applies to AGB stars with strong mass loss leading to very red infrared colors. The velocities and mean flux density levels have not changed since their discovery. As the minimum lifetime is of the same order as the wind crossing time, strong variations in the mass-loss process affecting the excitation conditions on timescales of ≈ 3000 years or less are unlikely.

Key words. stars: AGB and post-AGB – circumstellar matter – masers

1. Introduction

Molecular OH maser emission at 1612 MHz is frequently observed from stars approaching the tip of their evolutionary track on the asymptotic giant branch (AGB). These stars are in general long-period variables with pulsation periods >1 year. The pulsation is accompanied by heavy mass loss, which forms a circumstellar envelope (CSE) of gas and dust, and if the mass-loss rate surpasses $\dot{M} \approx 10^{-6}\ M_{\odot}\ \mathrm{yr}^{-1}$ the dust envelope becomes opaque for visible light. Classically these "invisible" stars were called OH/IR stars, but nowadays this term is often used in general reference to OH emitting AGB stars selected in the infrared (see review by Habing 1996).

Interestingly, a large fraction ($\approx 40\%$) of any sample of IRAS sources, selected to match the infrared colors of known OH/IR stars, does not exhibit a detectable OH 1612 MHz maser (Lewis 1992). These infrared sources were baptized by Lewis as "OH/IR star color mimics". Some of them do exhibit mainline OH (at 1665 or 1667 MHz) and/or 22 GHz H_2O masers (Lewis & Engels 1995), corroborating their cousinhood with OH/IR stars. OH/IR stars are therefore only part of the population of evolved and obscured AGB stars with oxygen-rich chemistry.

The reasons for the absence of 1612 MHz OH masers in a large fraction of oxygen-rich AGB stars are not known. The maser photons are emitted by a transition between hyperfine levels of the groundstate of OH, which are inverted with the help of pump photons at $\lambda = 35$ and 53 μm, emitted from dust in the CSEs. A requirement for excitation is sufficient OH column density, which might be low in mimics due to the destruction of OH by the interstellar UV field. This effect cannot account for mimics in general, as mimics are also present at higher galactic latitudes, where the influence of the UV field is low. In addition, the presence of a hot white dwarf companion leading to

photodissociation of OH is not generally able to suppress the OH maser (Howe & Rawlings 1994). A further requirement is velocity coherence over large distances to allow amplification. Turbulence may disrupt this coherence in the case of mimics.

An alternative explanation is the assumption that the OH maser is only present temporarily on the AGB and therefore these stars may change between an OH/IR status and that of a mimic. This explanation has been triggered by recent observations showing the fading of the OH maser in IRAS 18455+0448 over a time range of a decade (Lewis et al. 2001) and the absence of masers in four stars during a revisit of 328 OH/IR stars 12 years after their first detection (Lewis 2002). The high rate of "dead" OH/IR stars among a sub-sample of 112 OH/IR stars with relatively blue colors led Lewis to conclude that the mean 1612 MHz emission life is in the range 100–400 years.

To test this lifetime we reobserved another sample of $N > 100$ OH/IR stars, which was drawn from the first surveys for OH maser emission prior to 1980. With a difference of almost 30 years between the two observations several masers were expected to have disappeared.

2. Observations

The sample of OH/IR stars was mainly taken from the compilation of Baud et al. (1981), which contains $N = 114$ OH maser sources located at $10° \leq l \leq 150°, |b| \leq 4.2°$. Their source, OH 57.5+1.8, was found by Engels (1996) to be a blend of two OH masers and is included here as two objects, OH 57.5+1.8A and B. In addition, OH 19.2−1.0 was added, which was omitted by Baud et al. because of its peculiar maser profile. The full sample contained $N = 116$ objects and is listed in Table 1. The compilation of Baud et al. contains only masers that were discovered before 1978.

To ensure that a non-detection would not be caused by inaccurate coordinates, we compiled the literature for the best

---

[*] *Present address*: Observatorio Astronomico Nacional, Apartado 112, 28803 Alcala de Henares, Spain.

Table 1. OH/IR star sample and 1612 MHz OH maser properties.

Object	Coordinates (2000)		v_b [km s^{-1}]	SI$_b$ [Jy*km s^{-1}]	v_r [km s^{-1}]	SI$_r$ [Jy*km s^{-1}]	Comments
OH 10.5+4.5[a]	17 51 48.8	−17 42 30	−72.2	3.3	−42.5	2.8	
OH 10.9+1.5	18 03 38.9	−18 41 10	111.2	1.7	145.2	0.7	
OH 11.5+0.1	18 10 38.7	−18 52 57	10.1	23.1	75.1	130.9	
OH 12.3−0.2	18 13 08.8	−18 27 49	21.4	9.7	51.4	11.8	
OH 12.8−0.9	18 16 49.3	−18 15 02	−68.9	4.5	−43.1	5.5	
OH 12.8+0.9	18 10 06.1	−17 26 34	15.1	3.6	37.1	0.8	
OH 12.8−1.9	18 20 37.0	−18 47 11	−12.8	33.4	35.1	15.6	
OH 13.1+5.0	17 55 45.1	−15 03 42	−85.3	13.8	−47.3	6.0	
OH 13.4+0.8	18 12 03.4	−16 55 31	−22.5	1.2	15.4	3.4	
OH 15.4−0.1	18 18 54.0	−15 34 39	−44.6	3.1	−12.4	4.2	
OH 15.4+1.9	18 11 34.0	−14 39 54	−3.4	5.3	27.2	3.6	
OH 15.7+0.8	18 16 25.7	−14 55 15	−16.7	44.0	15.1	33.7	
OH 16.1−0.3	18 21 06.9	−15 03 22	−3.1	45.1	44.4	41.9	
OH 16.1+1.4	18 14 51.5	−14 16 19	28.3	1.0	66.5	0.7	
OH 17.0−0.1	18 21 49.9	−14 10 35	32.2	6.6	68.1	4.9	
OH 17.1−1.2	18 26 15.7	−14 42 26	−9.8	3.9	17.6	4.1	
OH 17.2−1.1	18 26 10.4	−14 28 19	157.2	1.3	184.2	1.7	
OH 17.4−0.3	18 23 35.0	−13 55 50	10.5	12.0	47.2	6.9	
OH 17.7−2.0	18 30 30.7	−14 28 58	46.4	52.2	75.1	131.0	
OH 18.2+0.5	18 21 56.2	−12 55 22	111.9	1.8	138.4	2.4	
OH 18.3+0.1[a]	18 23 50.8	−12 50 38	9.8	−	−	−	interstellar
OH 18.3+0.4	18 22 43.1	−12 47 42	31.3	8.5	64.3	10.3	
OH 18.5+1.4	18 19 35.5	−12 08 09	164.6	10.4	187.8	9.4	
OH 18.7+1.6	18 19 40.6	−11 53 00	−18.1	2.9	16.2	1.8	
OH 18.8+0.4	18 24 05.3	−12 26 14	−3.5	38.9	28.4	22.9	
OH 19.2−1.0	18 29 28.6	−12 37 55	29.9	8.4	68.3	12.7	
OH 19.5+4.0	18 12 22.7	−10 02 50	28.5	3.3	62.6	4.6	
OH 20.2−0.1	18 28 13.9	−11 16 10	8.5	10.2	44.3	8.8	
OH 20.3−1.5	18 33 34.2	−11 56 45	−25.1	1.7	2.2	3.1	
OH 20.4−0.3	18 29 35.5	−11 15 54	−	−	60.3	−	
OH 20.4+1.4	18 23 28.7	−10 27 21	19.4	0.8	57.0	0.7	
OH 20.6+0.3	18 27 56.3	−10 46 54	69.5	2.6	112.2	2.7	
OH 20.7+0.1	18 28 30.8	−10 50 52	116.9	20.3	155.7	14.2	
OH 20.8−0.8	18 31 23.0	−11 09 54	30.3	0.9	64.9	2.6	
OH 20.8+3.1	18 17 58.5	−09 18 31	11.2	3.7	41.5	4.4	
OH 21.5+0.5	18 28 30.9	−09 58 15	95.2	24.6	135.6	18.0	
OH 21.9+0.4	18 29 30.7	−09 39 50	65.8	4.8	105.9	3.6	
OH 22.1−0.6	18 33 34.5	−09 57 36	102.4	6.9	131.1	3.1	
OH 22.3−2.5	18 40 38.5	−10 42 35	97.5	1.2	126.9	1.4	
OH 23.1−0.3	18 34 11.3	−08 58 02	18.7	12.8	50.6	11.7	
OH 23.7+1.2	18 30 06.9	−07 36 50	−15.6	8.4	15.9	6.3	
OH 23.8+0.2	18 33 49.6	−08 04 01	93.3	3.5	118.0	9.0	
OH 23.8−1.1	18 38 39.8	−08 41 12	32.4	2.9	66.8	7.8	
OH 24.3+0.7	18 33 09.8	−07 27 58	39.3	1.8	75.8	2.4	
OH 24.5+0.3	18 35 19.0	−07 19 23	−87.3	6.8	−58.1	6.6	
OH 24.7−0.1	18 36 45.9	−07 18 17	60.3	5.3	110.8	7.7	
OH 24.7+0.1	18 35 57.4	−07 18 57	39.3	5.1	73.3	4.8	
OH 24.7+0.3	18 35 29.2	−07 13 11	19.8	12.8	65.0	14.8	
OH 24.7−1.7	18 42 22.0	−08 05 00	77.0	3.1	106.3	3.1	
OH 25.1−0.3	18 38 15.4	−07 09 54	128.7	4.8	156.2	4.1	
OH 25.5−0.3	18 38 50.5	−06 44 50	8.4	8.3	77.0	14.7	
OH 25.5+0.4	18 36 44.0	−06 27 24	21.4	4.7	56.2	3.1	
OH 26.2−0.6	18 41 14.4	−06 15 01	48.4	23.9	95.3	20.3	
OH 26.3+0.1	18 38 38.8	−05 49 10	−41.7	1.4	−11.2	1.8	
OH 26.4−1.9	18 46 26.8	−06 40 33	13.9	9.6	44.9	17.3	
OH 26.4−2.8	18 49 16.8	−07 13 47	−79.7	3.4	−53.3	3.6	
OH 26.5+0.6	18 37 32.5	−05 23 59	10.5	139.4	43.5	237.9	
OH 27.0−0.4	18 42 01.9	−05 21 07	86.0	5.2	117.7	7.0	

available radio coordinates and coordinates for their infrared counterparts. The original coordinates could have been wrong by several arc minutes, and not for all sources improved radio coordinates were later obtained by follow-up observations. Infrared counterparts (IRAS, MSX) were found for N = 113 OH maser sources, while there are no convincing counterparts for OH 18.3+0.1, OH 39.6+0.9, and OH 42.8−1.0. In the case of OH 18.3+0.1, the absence of an infrared counterpart coincident with the accurate position given by Bowers & de Jong (1983) confirms the suspicion of Winnberg et al. (1981) that this maser

Table 1. continued.

Object	Coordinates (2000)		v_b [km s^{-1}]	SI$_b$ [Jy*km s^{-1}]	v_r [km s^{-1}]	SI$_r$ [Jy*km s^{-1}]	Comments
OH 27.2+0.2	18 40 16.4	−05 02 39	71.6	1.5	113.4	2.0	
OH 27.3+0.2	18 40 21.9	−04 57 11	36.3	38.8	64.5	19.7	
OH 27.5−0.9	18 44 41.6	−05 09 18	92.1	7.1	121.2	9.1	
OH 27.8−1.5	18 47 37.8	−05 11 08	67.8	2.6	102.2	2.8	
OH 28.5−0.0	18 43 25.8	−03 55 55	92.9	13.8	122.0	13.8	
OH 28.7−0.6	18 45 48.3	−04 00 46	27.6	8.5	65.1	4.8	
OH 29.4−0.8	18 47 49.9	−03 29 31	106.1	17.0	140.1	16.3	
OH 30.1−0.2	18 47 09.8	−02 35 36	31.4	16.8	69.5	16.4	
OH 30.1−0.7	18 48 42.0	−02 50 29	76.8	65.8	121.2	79.9	
OH 30.7+0.4	18 45 52.4	−01 46 43	47.8	10.0	85.2	7.6	
OH 31.0+0.0	18 47 41.2	−01 45 11	26.7	0.2	41.7	12.9	
OH 31.0−0.2	18 48 43.1	−01 48 30	110.0	45.8	140.0	3.9	
OH 31.5−0.1	18 49 05.0	−01 17 02	19.4	3.3	50.9	2.8	
OH 31.7−0.8	18 52 01.4	−01 26 47	64.8	1.3	92.8	2.1	
OH 32.0−0.5	18 51 26.2	−01 03 52	54.0	24.5	98.2	13.8	
OH 32.1+0.9	18 46 38.7	−00 17 14	123.8	1.6	150.8	2.8	
OH 32.8−0.3	18 52 22.2	−00 14 11	42.9	55.8	78.5	26.8	
OH 33.4−0.0	18 52 27.9	+00 27 30	43.2	4.3	78.3	6.2	
OH 34.7+0.9	18 51 15.9	+01 56 19	10.2	4.2	44.6	5.1	
OH 34.9+0.8	18 52 15.3	+02 03 48	52.8	2.1	84.9	1.4	
OH 35.2−2.6	19 05 02.0	+00 48 51	21.3	21.8	73.8	15.8	
OH 35.6−0.3	18 57 27.4	+02 12 18	63.0	30.2	93.0	21.1	
OH 36.4+0.3	18 56 36.4	+03 06 53	82.2	3.3	122.4	2.9	
OH 36.9+1.3	18 54 16.0	+04 02 32	−20.8	3.4	−3.7	3.2	
OH 37.1−0.8	19 02 06.3	+03 20 16	73.0	10.7	103.9	9.1	
OH 37.7−1.4	19 05 09.7	+03 40 58	99.2	1.3	123.9	0.6	
OH 39.6+0.9A	19 00 55.5	+06 21 05		no detection			IRAS 18584+0616
OH 39.6+0.9B[b]	19 00 24.6	+06 16 31		no detection			IRAS 18579+0612
OH 39.7+1.5	18 58 30.1	+06 42 55	2.1	75.6	38.0	129.7	
OH 39.9−0.0	19 04 09.6	+06 13 16	132.9	10.6	165.0	11.3	
OH 40.1+2.4	18 55 56.9	+07 30 28	26.0	1.1	67.8	1.5	
OH 42.3−0.1	19 09 08.2	+08 16 34	41.4	22.7	77.6	41.8	
OH 42.6+0.0	19 08 58.4	+08 37 49	34.1	5.6	71.8	4.8	
OH 42.8−1.0[d]	19 13 36.4	+08 22 39	−29.5	2.2	−1.8	1.0	Pos. error: ≈2′
OH 43.6−0.5	19 12 46.9	+09 18 24	58.8	1.6	86.3	1.4	
OH 43.8+0.5	19 09 31.8	+09 51 50	−4.3	5.8	22.5	4.4	
OH 43.9−1.0	19 15 16.4	+09 15 45	37.8	0.8	65.5	1.1	
OH 43.9+1.2	19 06 42.8	+10 14 33	32.4	2.0	67.4	1.5	
OH 44.8−2.3	19 21 36.6	+09 27 57	−88.9	10.1	−53.8	14.4	
OH 45.5+0.1	19 14 19.6	+11 10 35	16.5	14.9	53.7	14.2	
OH 51.8−0.2	19 27 42.1	+16 37 25	−18.5	7.3	23.1	5.4	
OH 52.4+1.8	19 21 31.5	+18 10 09	−0.3	2.7	31.3	4.5	
OH 53.6−0.2	19 31 25.3	+18 13 10	−4.0	9.8	25.5	23.9	
OH 55.0+0.7	19 30 29.4	+19 50 41	12.5	14.8	44.2	9.3	
OH 57.5+1.8A	19 31 38.9	+22 35 17	−88.0	1.9	−59.2	1.6	
OH 57.5+1.8B	19 31 45.5	+22 33 42	30.1	2.2	46.3	4.8	
OH 63.9−0.2	19 52 57.9	+27 07 45	−11.3	1.7	22.3	1.8	
OH 65.5+1.3	19 51 21.2	+29 13 01	−41.1	6.9	−2.7	6.6	
OH 65.7−0.8	19 59 39.4	+28 23 10	−70.2	2.4	−46.1	4.0	
OH 66.8−1.3	20 04 20.8	+29 04 07	−79.1	2.6	−50.2	2.7	
OH 75.3−1.8	20 29 08.5	+35 45 42	−16.4	3.7	10.0	3.7	
OH 77.9+0.2	20 28 30.7	+39 07 00	−50.9	8.5	−26.0	5.6	
OH 80.8−1.9	20 46 25.5	+40 06 58	−28.7	1151.4	25.6	215.5	
OH 83.4−0.9	20 50 58.6	+42 48 12	−58.1	11.6	−18.1	5.2	
OH 85.4+0.1	20 53 38.0	+44 58 07	−36.8	3.0	−7.9	2.8	
OH 104.9+2.4	22 19 27.2	+59 51 20	−41.3	36.3	−8.5	26.5	
OH 127.8+0.0	01 33 51.2	+62 26 53	−66.5	67.3	−41.8	40.9	
OH 138.0+7.2[c]	03 25 08.4	+65 32 07	−47.7	18.5	−26.5	8.9	
OH 141.7+3.5[c]	03 33 30.5	+60 20 09	−70.2	4.9	−43.7	1.7	

Coordinates: a) Bowers & de Jong (1983); b) IRAS; c) Bowers et al. (1981); d) this paper; otherwise MSX6C.

is actually of interstellar nature. OH 39.6+0.9 was discovered by Johansson et al. (1977), which gave an error of rms = 2″5 for its position. The source was never reobserved. The nearest IRAS counterparts are IRAS 18578+0616 and 18584+0616, with a distance of 4′3. OH 42.8−1.0 has also never been reobserved since its discovery by Baud et al. (1979). The positional

error of the discovery position is rms $\approx 3'$. IRAS 19108+0815 is the nearest IRAS counterpart, with a distance of 2.4. The IRAS source is weak and was not detected by MSX. We also suspected that OH 39.6+0.9 and OH 42.8−1.0 are not OH/IR stars. Nevertheless, all three sources were reobserved.

The observations were made during two nights 2005, August 2–4 with the Effelsberg radio telescope. As frontend we used the 1.3–1.7 GHz HEMT receiver and as backend an 8192 channel autocorrelator. The correlator was split into four segments, of which three were centered on the two OH main line frequencies 1665.401 and 1667.359 MHz and one on the OH satellite line frequency 1612.231 MHz. The fourth segment was not used because of technical problems. In this paper we focus on the results of the 1612 MHz observations, for which the receiver passed left circular polarization. We chose a bandwidth of 1.25 MHz, yielding a velocity resolution of 0.11 km s^{-1} and a velocity coverage of ± 112.5 km s^{-1}, centered on the mean velocity of the two OH maser lines, as given by Baud et al. (1981). The beamwidth was 7.8. The coordinates to which the telescope was pointed are given in Table 1. If not otherwise stated, they were taken from the MSX6C catalog. The errors of all coordinates are smaller than a few arcsec, and therefore much smaller than the beamwidth. System temperatures were ≈ 25 K at zenith. We observed in position switch mode with an integration time of 6 min (ON+OFF), yielding a typical sensitivity of 0.25 Jy (3σ).

The data reduction was made within CLASS and included removal of the baseline and flux calibration. The calibration was made against 3C 286 and 3C 48 adopting flux densities of 13.53 ± 0.05 Jy and 14.25 ± 0.05 Jy, respectively (Ott et al. 1994). No gain curve was applied as the flux calibrators were observed several times during the nights and showed no elevation dependent variations over the $20-70°$ elevation range observed.

3. Results

We recovered the masers for all 113 OH maser sources with infrared counterparts. In general, velocities and flux densities were compatible with the values given by Baud et al. (1981). Table 1 lists the ends v_b and v_r of the full velocity range, over which emission was detected, and the integrated flux densities SI_b and SI_r. We adopted the midpoint of the velocity range $v_b - v_r$ as radial velocity $v_\star$ of the star. The integrated flux densities SI_b and SI_r were determined by integrating the calibrated spectra over the two halves of the velocity range $v_\star - v_b$ and $v_r - v_\star$.

Figure 1 shows a comparison of the velocities between our data and the values listed by Baud et al. (1981). Within the errors $(\pm 2$ km s$^{-1})$ there is good agreement between the velocities. In a few sources, weak emission was found outside the main peaks, which led to radial velocities deviating by as much as 7 km s^{-1} from the previous values. OH 24.7−0.1 and OH 20.4−0.3 are not included in the figure. In the case of OH 24.7−0.1 (cf. Fig. 2), the velocities needed a complete revision. In the discovery paper of this source (Johansson et al. 1977), only the stronger of the two lines at ≈ 111 km s^{-1} was clearly detected, while a marginal feature at ≈ 142 was considered as the second line. The new spectrum shows that the second line is at the lower velocity of 62 km s^{-1}. In OH 20.4−0.3 we could not measure v_* because the blue emission peak was corrupted by interference.

Figure 3 shows a comparison of the integrated flux densities. The scatter is largely within the margins expected from the large amplitude variations due to the pulsations of the star. Typical variations have a factor of about 2.5 (Herman & Habing 1985).
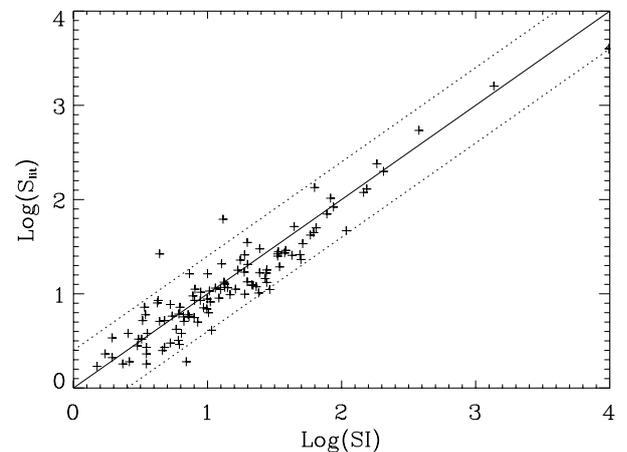
Mixed results were obtained for the three maser sources without IRAS/MSX counterparts. For OH 18.3+0.1 we found
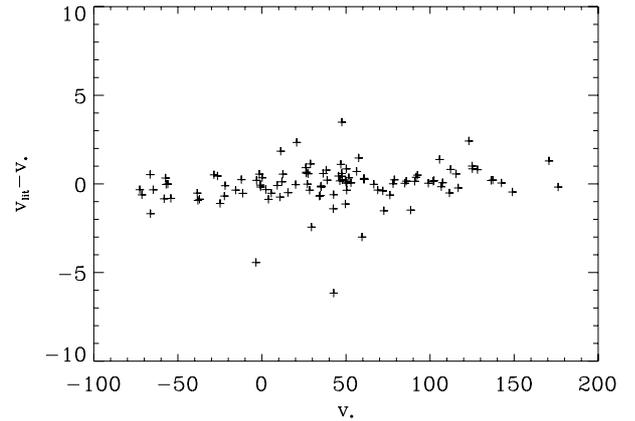
Fig. 1. Deviations of measured radial velocities $v_\star$ of the OH/IR stars observed from radial velocities v_{lit} given by Baud et al. (1981).
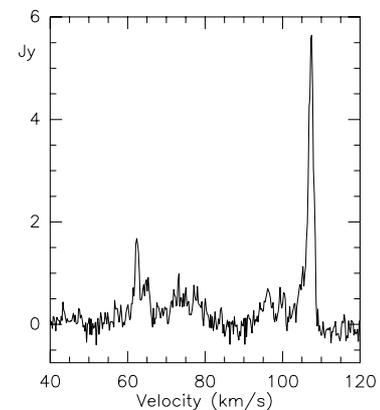
Fig. 2. 1612 MHz OH maser spectrum of OH 24.7−0.1.

Fig. 3. Comparison of measured integrated flux densities $SI = SI_b + SI_r$ of the OH/IR stars observed with flux densities S_{lit} given by Baud et al. (1981). The units are 10^{-22} Watt m^{-2}. The dashed lines delimit the deviations expected due to flux variations by a factor 2.5.

a single line at 9.8 km s^{-1} (3 Jy), which possibly belongs to the interstellar maser line at +11 km s^{-1}, discussed by Baud et al. (1979). For OH 39.6+0.9 we searched for the maser in a $15' \times 15'$ region around the position of the two nearest IRAS sources, after no OH masers were detected at the IRAS positions themselves. No maser could be found down to 0.8 Jy (3σ). OH 42.8−1.0 was detected (Fig. 4). To improve the coordinates we tried to maximize the signal. The improved position is
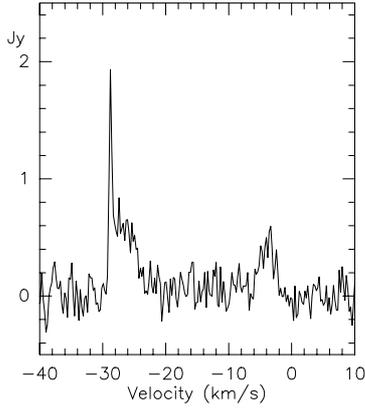
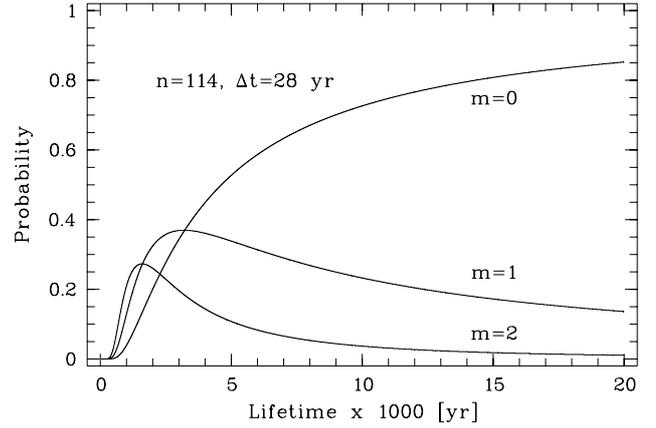**Fig. 4.** 1612 MHz OH maser spectrum of OH 42.8−1.0.

Fig. 5. Probabilities P_n^m that out of $n = 114$ OH masers, m masers with a lifetime T will have disappeared after $\Delta t = 28$ years.

Table 2. Lower lifetime limits $T_{\min}$ at different significance levels for 1612 MHz OH masers based on observations in this paper. P_n^m is the probability for finding exactly m extinguished maser among n stars re-observed after Δt years.

n	m	Δt [yr]	$T_{\min}$ [yr]	P_n^m [%]	Comments	
114	0	28	550	0.2	3σ	This paper
114	0	28	1050	4.6	2σ	
114	0	28	2800	31.8	1σ	

$\alpha = 19^{\mathrm{h}}13^{\mathrm{m}}36.4^{\mathrm{s}}$ (±5.0s), $\delta = +08° 22' 39''$ (±2'). The position is still too coarse to allow an unambiguous identification with an infrared source. The most likely candidate is IRAS 19112+0816, which is approximately 1' away.

To summarize, the only sources from the sample of OH/IR stars of Baud et al. (1981), that we did not redetect at all, or not at the expected velocities, are OH 18.3+0.1 and OH 39.6+0.9. They are two of the three objects for which no infrared counterpart was found. We therefore conclude that these two sources are not OH/IR stars, while for the third, OH 42.8−1.0, the classification as OH/IR star is retained. We further summarize that all OH/IR stars in the sample ($N = 113 +$ OH 42.8−1.0) still possess an 1612 MHz OH maser. As these stars were discovered prior to 1978, we adopt $\Delta t = 28$ years as the minimum time passed between discovery and redetection in 2005.

4. Lifetime of OH masers

The restrictions on the lifetime of OH masers following from the redetection of all bona-fide OH/IR stars, can be accessed using a basic law of combinatorics.

We will assume that stars enter at random times into the phase where they support maser emission. We assume also that the mean lifetime of an OH maser in a CSE is T years, and a known OH maser is revisited after Δt years and has disappeared. Assuming $\Delta t < T$, the probability to disappear is $\Delta t/T$ and the probability to detect a maser again is $(1 - \Delta t/T)$.

If a sample of n OH masers is revisited and all are redetected, the accumulated probability P_n^0 that no maser disappeared within Δt years is

$$P_n^0 = \left(1 - \frac{\Delta t}{T}\right)^n. \tag{1}$$

The probability to detect the disappearance of a single maser is

$$P_n^1 = n \cdot \left(\frac{\Delta t}{T}\right) \cdot \left(1 - \frac{\Delta t}{T}\right)^{n-1} \tag{2}$$

where the factor n allows for the fact that any of the n masers might have been affected.

More general, the probability to detect the disappearance of m masers among n stars after Δt years is

$$P_n^m = \frac{n!}{m!(n-m)!} \cdot \left(\frac{\Delta t}{T}\right)^m \cdot \left(1 - \frac{\Delta t}{T}\right)^{n-m}. \tag{3}$$

This general equation (a standard relation in combinatorics) includes the case that no maser ($m = 0$) disappeared, or that all

of them are extinguished ($m = n$), e.g., the valid range for m is $0 \le m \le n$.

In Fig. 5 we plot the probabilities derived from Eq. (3) for the case $n = 114$ stars, $m = 0-2$ missing masers, and $\Delta t = 28$ years for lifetimes T up to 20 000 years. The curves tell us for $T = 15\,000$ years, for example, that the probability to redetect all masers is 81%, and that there is a 17% chance of observing one star with an extinguished maser. Even the non-detection of two masers is non-negligible: 2%. For smaller lifetimes, say $T < 5000$ years, the cumulative probability for $m \le 2$ does not approach 100%, because now the disappearance of $m > 2$ masers is not unlikely anymore.

As expected, the probability to redetect all masers decreases towards lower lifetimes. There is no absolute lower lifetime limit, but it is possible to define such limits in relation to significance levels. For example, lifetimes T in which the probability of finding *at least* one maser extinguished exceeds 68.2%, can be excluded at the 1σ level. The probability of finding *at least* one extinguished maser is $(1 - P_{114}^0)$, which is different from the probability P_{114}^1 (Eq. (2)) for finding *exactly* one extinguished maser. For our sample, probabilities $(1 - P_{114}^0) > 0.682$ or $P_{114}^0 < 0.318$ to detect an extinguished maser are obtained for lifetimes $T \lesssim 2800$ years (Fig. 5). As all masers were redetected, $T_{\min} = 2800$ years is a lower limit of the lifetime at the 1σ level. Lower lifetime limits with higher significance levels are given in Table 2. Lifetimes of $T < 400$ years, as derived by Lewis (2002), have $P_{114}^0 < 0.01$ and can be excluded for our sample.

5. Discussion

The high rate of extinguished masers in the sample studied by Lewis (2002) (Arecibo sample) is at odds with our results. The rate is also astonishing given that previous monitoring programs did not witness similar maser luminosity fading processes over

periods of several years. On the other hand, a disappearance of masers in our sample would not have been too surprising. For one part of the sample, drastic mass-loss variations due to the onset of a "superwind" a few hundred years ago was postulated (Justtanont et al. 2006), and another part of the sample belongs to the group of "non-variable OH/IR stars", for which a loss of their masers within a couple of thousand years is predicted (Engels 2002).

5.1. Lifetime limit derived from the Arecibo sample

Before discussing possible causes due to the different sample properties, we will have a look at the restrictions on lifetimes for the Arecibo sample using the equations of the previous section. Lewis (2002) concluded that after $\Delta t = 14$ years, from $n = 112$ stars, five masers will have disappeared. The affected stars are the IRAS objects 15060+0947, 18455+0448, 19479+2111, 19529+3634, and 20547+0247. He argues that the most likely lifetime is $T = 314(-97, +387)$ years. The maser in IRAS 15060+0947, which was steadily declining at the time of the Lewis (2002) publication, actually never completely disappeared. Another one, IRAS 19479+2111, reappeared in 2005 (Lewis, priv. communication). The probable lifetime of masers in the Arecibo sample is therefore certainly longer than the $T = 314$ years.

We will ask here the probability of finding m or more extinguished masers for a given lifetime. This allows the determination of upper limits for the OH maser lifetimes in the Arecibo sample at different significance levels. For the purpose of this calculation, we will use $m = 4$ extinguished masers (omitting IRAS 15060+0947) and make an adjustment to $\Delta t = 12$ years.

The probability of finding at least m masers extinguished among n stars after Δt years is

$$Q_n^m = \sum_{i=m}^{n} P_n^i. \qquad (4)$$

For $m = 1$, the case discussed in the previous section, one finds

$$Q_n^1 = \sum_{i=1}^{n} P_n^i = \sum_{i=0}^{n} P_n^i - P_n^0 = 1 - P_n^0. \qquad (5)$$

The probability Q_{112}^4 is plotted as a function of T in Fig. 6. This probability drops below 31.2% at $T = 476$ years, meaning the exclusion of longer lifetimes at the 1σ-level. Lifetimes $T \gtrsim 2400$ years can be safely excluded, as the probability falls below 0.2% (3σ) (Table 3).

Thus, the high rate of extinguished masers in the Arecibo sample indeed points to rather short lifetimes, while in our sample, similar short lifetimes are unlikely. However, as Lewis (2002) already pointed out, the two samples cannot be compared directly, because the stars with extinguished masers mostly belong to a population of OH/IR stars with low main-sequence masses, blue IRAS colors, periods $P < 700$ days, and envelope expansion velocities $v_e < 12$ km s^{-1}, which have to be distinguished from the *classical* OH/IR stars observed here. The latter have larger progenitor masses, redder IRAS colors, periods 1000–2000 days, and $v_e > 12$ km s^{-1}. The classical OH/IR stars have larger mass-loss rates and probably create CSEs, providing an environment more favorable for OH maser emission. The higher stability of their masers may then be responsible for the longer lifetimes compared to those hosted by the less dense envelopes of the bluer OH/IR stars.
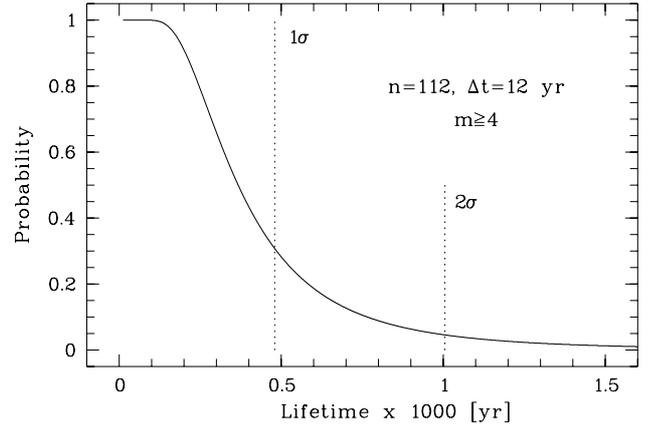
Fig. 6. Probabilities Q_{112}^4 that out of $n = 112$ OH masers, $m \geq 4$ masers with a lifetime T will have disappeared after $\Delta t = 12$ years. The vertical lines mark the upper lifetime limits $T_{\max}$ at the 1σ and 2σ-level significance.

Table 3. Upper lifetime limits $T_{\max}$ at different significance levels for 1612 MHz OH masers, based on observations of the Arecibo sample. Q_n^m is the probability for finding at least m extinguished masers among n stars reobserved after Δt years.

n	m	Δt [yr]	$T_{\max}$ [yr]	Q_n^m [%]	Comments	
112	4	12	2410	0.2	3σ	Arecibo
112	4	12	1005	4.6	2σ	sample
112	4	12	476	31.2	1σ	

5.2. Monitoring programs

In line with our results, thus far, no extinction of an OH maser has been reported from monitoring programs. The longest was carried out over 15 years by Etoka & Le Squeren (2000), but contained only 7 Mira variables, which are IRAS sources with blue colors. A larger number of OH/IR stars ($n = 37$) was covered by van Langevelde et al. (1993), however the monitoring time was only 3 years. 1σ lower limits $T_{\min} \approx 100$ years for these samples do not give useful lifetime constraints. A larger sample containing 60 OH/IR stars was monitored over 10 years by Herman & Habing (1985) and van Langevelde et al. (1990), but it is a subsample of the present one studied here, and therefore gives no independent information.

5.3. A recent onset of a "superwind"?

Drastic changes of the excitation conditions for OH masers on timescales of hundreds of years is implied by the two wind regime, invoked by Justtanont et al. (1996) to model the CSE of the classical OH/IR star OH 26.5+0.6. This object is a prototype OH/IR star and part of our sample. Their model consisted of an inner "superwind" and an outer more tenuous AGB wind (hosting the OH maser). The transition to the 550 times higher mass-loss rates of the "superwind" lasted less than 150 years and started $\approx$200 years ago. Support for a generalization of this model to OH/IR stars has commonly been obtained from observations of water-ice (Justtanont et al. 2006). Water-ice is formed in the outer envelopes at radii $>10^{16}$ cm, and the difference between OH/IR stars with or without a water-ice absorption band at 3.1 μm might be related to the question, if the high dust densities of the "superwind" have already reached this region or not. Given the short timescales involved, one expects that, at least in

one star, the transition region between both winds has passed its OH maser shell during the last 30 years. However, no evidence comes from the flux level of the OH masers or their velocities that the excitation conditions of any of them (encompassing most of the stars studied by Justtanont et al.) have been changed due to a several hundred-fold increase of the density or the number of pump photons in their surroundings.

5.4. Non-variable OH/IR stars

For part of our sample, a lifetime of the OH masers of less than a few thousand years is predicted due to the dissipation of the CSE during transition to the post-AGB phase. Stars in this phase are distinguished by their non-variability and are called "non-variable OH/IR stars", with non-variability defined as absence of large-amplitude variations typical for Mira stars. The non-variable OH/IR stars are thought to have stopped their pulsations and the associated strong mass loss, and have therefore developed a hollow shell, which continues to expand. Inside, the densities will have dropped sharply and it takes $\lesssim 2000$ years for the inner boundary of this shell to reach the OH maser region, assuming a mean expansion velocity 12 km s^{-1} and a OH maser shell radius of several 10^{16} cm. The drop in density will ultimately extinguish the OH masers. Support for this scenario was given by Engels (2002), who reported the disappearance of the H_2O maser of OH 17.7−2.0 (a present sample member) within a decade. This extinction of the maser was attributed to the expected drop of densities in the H_2O maser zone, after which the inner boundary of the hollow shell passed. As H_2O masers in OH/IR stars are typically located ≈ 10 times closer to the star than OH masers, the extinction of the OH maser in OH 17.7−2.0 is expected to happen in the coming centuries. Also, the disappearance of the OH maser in IRAS 18455+0448, an Arecibo source with very red infrared colors, can be explained by its possible status as an emerging post-AGB star (Lewis et al. 2001).

Among our sample, 45 OH masers were monitored by Herman & Habing (1985) and they found 13 ($\approx 30\%$) of them with no or very weak (irregular) variations. Assuming that this fraction of non-variable objects is valid for our full sample, we find that the lifetime of the OH masers in non-variable OH/IR stars is >820 years (1σ). The re-detection of all OH masers is therefore still compatible with the classification of these stars as transition objects. On the other hand, Gray et al. (2005) modeled the decline of the OH maser emission after detachment of the CSE and found that the masers disappear even before the inner border of the detached envelope has reached the OH maser shell, because they depend on pumping photons that emerge from the dust further inside. Therefore, the decay of the masers starts immediately after detachment and is finished in their models within <100 years. To maintain the classification of the non-variable OH/IR stars as post-AGB stars, it is therefore mandatory to assume that the mass loss does not stop abruptly with the cessation of the large-amplitude variations at the end of the AGB evolution. The mass-loss rates more likely decline gradually over a time range of several thousand years.

5.5. Envelope properties and the stability of OH masers

Because of the rarity of masers in the post-AGB phase, masers in general will disappear with the end of AGB evolution. The OH/IR stars with bluer envelopes are however genuine AGB stars and therefore, the disappearance of their masers requires a different explanation. The traditional assumption is that the

timescales for which mass-loss rates change in response to evolutionary changes in the AGB (the intermittent thermal pulses) are much longer than the wind crossing times of a few thousand years through the CSE. Prior to departure from the AGB, there are only the phases during and after a thermal pulse in which shorter timescales are prevalent. Lewis (2002) therefore associates the observed short lifetimes of the OH masers in the lower-mass stars with a brief evolutionary phase after thermal pulses of duration ≈ 500 years, when mass-loss rates are sufficiently high to drive a wind able to host masers. The decline of the masers would then be a result of rapidly declining mass-loss rates.

We observed the infrared counterparts of most OH masers in the Arecibo sample (Jiménez-Esteban et al. 2005) and monitored them for several years, including the five stars discussed by Lewis (2002). IRAS 18455+0448 is non-variable, corroborating Lewis' conclusion that this star is already in the post-AGB phase. IRAS 20547+0247 (=U Equ) is also non-variable; this is known as a peculiar star surrounded by an edge-on disk or torus (Barnbaum et al. 1996), instead of a radial symmetric CSE. Thus, this star may not be representative of OH/IR stars in general. IRAS 15060+0947, as discussed by Lewis (2002), and the remaining two stars, IRAS 19479+2111 and IRAS 19529+3634, are large-amplitude variables. We did not find variations in the mean magnitudes or colors during the monitor period 1999–2005 for any of these stars, indicating that their mass-loss rates did not change strongly. Thus, there is no independent evidence for a change in the mass-loss process being a cause for the disappearance of the masers. Furthermore, the typical time a 1 $M_\odot$ star spends on the thermal pulsing AGB is of the order of 5×10^5 years (Vassiliadis & Wood 1993), with at least 10% of this time having sufficiently high mass-loss rates to be able to sustain a maser. With a OH maser detection rate of 60% (Lewis 1992) among IRAS selected AGB star samples, the expected lifetimes of OH masers are $\gtrsim 30\,000$ years, and therefore it is unlikely that the (temporary) disappearance of the masers in the bluer envelopes is linked to evolution. The reappearance of the OH maser in IRAS 19479+2111 after a couple of years indicates that the maser extinction in blue envelopes in general is not permanent, but rather a temporary effect.

The lack of evidence for major changes of the infrared properties precludes the lack of pumping photons as cause for the (temporary) extinction of the OH masers in blue envelopes. Variations of density or velocity coherence disruption remain as alternatives. One might envisage modulations of the mass-loss process on timescales of hundreds of years, which might suffice to affect the excitation conditions significantly. Such modulations of the envelope structure were found in studies of dust scattered light at distances up to $\gtrsim 10^{21}$ cm from the stars (Mauron & Huggins 2006). At such a range of distances, the history of the mass-loss process can be studied over $\approx 10\,000$ years. They find in the case of IRC+10216, a carbon star on the AGB, shells spaced at irregular intervals corresponding to timescales of 200–800 years (Mauron & Huggins 2000), showing the presence of modulation on the required timescales. In hydrodynamical models for dust driven AGB winds, Simis et al. (2001) found that such quasi-periodicity develops naturally in the winds, if dust and gas are not perfectly coupled. While the increase of densities probably associated with the shells would improve the excitation conditions for OH masers, an increase of turbulent motion would likely decrease the gain lengths.

If such modulations of the envelope structure are responsible for OH maser extinction, then the different lifetimes derived from the Arecibo sample and from the sample studied

here, point to a different susceptibility of their masers to the inferred changes of the excitation conditions. The masers in classical OH/IR stars, as studied in this paper, would be more robust against extinction than the ones in bluer envelopes. The inability to distinguish OH/IR stars and "OH/IR star mimics" by ways other than by their masers would then be explained by the instability of the OH masers, which turn on or off in response to variations of the envelope structure. The timescales of such variations would be of the order of ≲1000 years in the case of stars with blue envelopes and ≳3000 years for the reddest OH/IR stars. Any sample of oxygen-rich AGB stars would then show, at different times, a different set of stars exhibiting OH maser emission.

6. Conclusions

We find that the lifetime of OH masers in classical OH/IR stars is >2800 years, in contrast to the lifetime implied by the observed disappearance of several masers in AGB stars with bluer envelopes. The lower limit of the lifetime is of the order of the wind crossing time in the CSEs, implying that, in general, no drastic variations in the structure of the CSEs happen on such timescales, or shorter ones. If non-variable OH/IR stars are in transition to the post-AGB stage, a sudden decline of the mass-loss rates at the end of AGB evolution is ruled out. The previous observed disappearance of OH masers in stars with bluer envelopes is probably not associated with major changes in the mass-loss process. The susceptibility of masers to smaller variances in their environment may lead to OH masers as transient phenomena on the AGB. This gives a natural explanation for the detection of OH masers in only a part of any AGB star sample with otherwise similar properties.

References

Barnbaum, C., Omont, A., & Morris, M. 1996, A&A, 310, 259
Baud, B., Habing, H. J., Matthews, H. E., & Winnberg, A. 1979, A&AS, 36, 193
Baud, B., Habing, H. J., Matthews, H. E., & Winnberg, A. 1981, A&A, 95, 156
Bowers, P. F., & de Jong, T. 1983, AJ, 88, 655
Bowers, P. F., Johnston, K. J., & Spencer, J. H. 1981, Nature, 291, 382
Engels, D. 1996, A&A, 315, 521
Engels, D. 2002, A&A, 388, 252
Etoka, S., & Le Squeren, A. M. 2000, A&AS, 146, 179
Gray, M. D., Howe, D. A., & Lewis, B. M. 2005, MNRAS, 364, 795
Habing, H. J. 1996, A&AR, 7, 97
Herman, J., & Habing, H. J. 1985, A&AS, 59, 523
Howe, D. A., & Rawlings, J. M. C. 1994, MNRAS, 271, 1017
Jiménez-Esteban, F. M., Agudo-Mérida, L., Engels, D., & García-Lario, P. 2005, A&A, 431, 779
Johansson, L. E. B., Andersson, C., Goss, W. M., & Winnberg, A. 1977, A&AS, 28, 199
Justtanont, K., Skinner, C. J., Tielens, A. G. G. M., Meixner, M., & Baas, F. 1996, ApJ, 456, 337
Justtanont, K., Olofsson, G., Dijkstra, C., & Meyer, A. W. 2006, A&A, 450, 1051
Lewis, B. M. 1992, ApJ, 396, 251
Lewis, B. M. 2002, ApJ, 576, 445
Lewis, B. M., & Engels, D. 1995, MNRAS, 274, 439
Lewis, B. M., Oppenheimer, B. D., & Daubar, I. J. 2001, ApJ, 548, L77
Mauron, N., & Huggins, P. J. 2000, A&A, 359, 707
Mauron, N., & Huggins, P. J. 2006, A&A, 452, 257
Ott, M., Witzel, A., Quirrenbach, A., et al. 1994, A&A, 284, 331
Simis, Y. J. W., Icke, V., & Dominik, C. 2001, A&A, 371, 205
van Langevelde, H. J., van der Heiden, R., & van Schooneveld, C. 1990, A&A, 239, 193
van Langevelde, H. J., Janssens, A. M., Goss, W. M., Habing, H. J., & Winnberg, A. 1993, A&AS, 101, 109
Vassiliadis, E., & Wood, P. R. 1993, ApJ, 413, 641
Winnberg, A., Terzides, Ch., & Matthews, H. E. 1981, AJ, 86, 410